3046 © 1991 The Chemical Society of Japan Bull. Chem. Soc. Jpn., 64, 3046—3058 (1991) [Vol. 64, No. 10

Structural, Magnetic, and Spectroscopic Characterization of the Pyridine Complexes of Copper(II) Triphenylacetate: A Dimeric Copper(II) Triphenylacetate–Pyridine Complex with Distorted Trigonal Bipyramidal Geometry Around Copper[1)]

Omar W. Steward,* Michinobu Kato,*,† Shih-Chi Chang, Martin Sax,†† Chong-Hwan Chang,††
C. Frederick Jury, Yoneichiro Muto,††† Tadashi Tokii,††† Toshiaki Taura,†
James F. Pletcher,†† and Chung Soo Yoo††
Department of Chemistry and Physics, Duquesne University, Pittsburgh, Pennsylvania 15282, U.S.A.
†Department of Chemistry, Aichi Prefectural University, Mizuho-ku, Nagoya 467
††Biocrystallography Laboratory, V A Medical Center, Pittsburgh, Pennsylvania 15240 and Department of Crystallography, University of Pittsburgh, Pittsburgh, Pennsylvania 15260 U.S.A.
†††Department of Chemistry, Faculty of Science and Engineering, Saga University, Saga 840

(Received March 11, 1991)

The synthesis and characterization of three copper(II) triphenylacetate–pyridine complexes are reported along with their magnetic and spectral properties: $[Cu_2(O_2CCPh_3)_4(py)_2]\cdot C_6H_6$ (**1**), $[Cu_2(O_2CCPh_3)_4(py)_2]$ (**2**), and $Cu(O_2CCPh_3)_2\cdot 2py$ (**3**). Crystal structure analyses of **1** and **3** have revealed unusual geometries around copper: **1**, triclinic, space group $P\bar{1}$ with a=19.558(7) b=16.605(6), c=14.997(5) Å, α=114.55(2)°, β=97.11(2)°, γ=111.65(2)°, and Z=2; **3**, monoclinic, space group $P2_1/c$ with a=8.931(1), b=12.602(1), c=19.578(1) Å, β=118.17(0.4)°, and Z=2. The coordination sphere around each copper in the dimeric complex **1** is a highly distorted trigonal bipyramid with bridging triphenylacetato ligands spanning the apical and equatorial positions, resulting in a long Cu–Cu distance of 3.086(1) Å. Temperature-dependent magntic susceptibility measurements on **1** indicate that the two coppers are antiferromagnetically coupled with $-2J$=187 cm^{-1}. The structure of the monomeric complex **3** is unusual in that the out-of-plane carboxylate oxygen is twisted 12° from the normal. Two solid modifications are observed for **2**. The magnetic and spectral properties of **2a** ($-2J$=173 cm^{-1}) resemble those of **1**, and **2b** ($-2J$=321 cm^{-1}) those of copper(II) acetate monohydrate. Magneto-structural correlations are presented. The novel structural features of these complexes are suggested to arise from steric effects resulting from the spatial relationships both between and within the molecules in the crystal environment.

The structures of a large number of dimeric copper(II) complexes with the formula $[Cu_2(O_2CR)_4(L)_2]$, where R is an organic group and L is a Lewis base, have been determined.[2—6] Almost all of these complexes have the classical copper(II) acetate monohydrate-type structure in which the ligand atoms in the coordination sphere around copper(II) are located near the corners of a square pyramid. Recently, some members of two families of these complexes have been observed to have a variation of this structure, in which the arrangement of the ligands around copper(II) can best be described as being distorted trigonal bipyramidal: complexes with bridging triphenylacetato ligands[7—10] and complexes with bridging trichloroacetato ligands.[10—16]

In this paper we report on the first complete structural analysis of a complex from the family containing triphenylacetato ligands, [tetrakis(μ-triphenylacetato-*O,O'*)bis(pyridine)dicopper(II)]–benzene(1/1), $[Cu_2(O_2CCPh_3)_4(py)_2]\cdot C_6H_6$ (**1**). In **1**, the coordination geometry around each of the two copper atoms is that of a highly distorted trigonal bipyramid. The factors which cause the unusual geometry around copper(II) in this binuclear complex are attributed to steric effects resulting from the spatial relationships both between and within the molecules in the crystal environment, the former being of prime importance.

Two different solid modifications of the dimeric complex, [tetrakis(μ-triphenylacetato-*O,O'*)bis(pyridine)dicopper(II)], $[Cu_2(O_2CCPh_3)_4(py)_2]$ (**2a** and **2b**), have been prepared and found to exhibit different magnetic and spectral properties. We report on the first study concerning the effect of the ligand arrangement around copper, distorted trigonal bipyramidal and square pyramidal, on the magnetic and spectral properties of these binulear conformers.

The conversion of **1** to *trans*-bis(triphenylacetato-*O,O'*)bis(pyridine)copper(II), $Cu(O_2CCPh_3)_2\cdot 2py$ (**3**), in the crystalline state is discussed. The crystal structure of the monomeric complex **3** reveals a structural modification from the reported structures for complexes of the type $Cu(O_2CR)_2\cdot 2L$, where L represents a nitrogeneous base, resulting from steric effects in which the out-of-plane carboxylate oxygen is twisted 12° from the normal. The so-called "dimer spectral band", which is observed for the complexes **1**, **2a**, and **2b**, is not observed for **3**.

Experimetal

General Procedures. All calculations for copper(II) carboxylates are based on formula weights, unless indicated otherwise. Analyses were performed by Analytische Laboratorien, Elbach, West Germany, with the exception of some copper analyses that were performed in our laboratories by atomic absorption and EDTA titration.

Materials. The starting materials (and sources) are as follows: triphenylacetic acid, benzene-d_6, ethanol-d (Aldrich Chemical Co.); copper(II) acetate monohydrate, pyridine (Fisher Scientific Co.).

Preparation of the Complexes. (a) $[Cu_2(O_2CCPh_3)_4(py)_2]\cdot C_6H_6$ (1) Crystals. A Büchner funnel with a fritted disk (30 mL-30 M) was placed in a beaker (100 mL). A melting-point tube open at both ends was bent and then inserted so that the air pocket which formed under the filter could be minimized. Into the beaker was added a solution of absolute ethanol–pyridine (50 : 1 v/v). $Cu(O_2CCPh_3)_2\cdot 2H_2O$ (0.3 g, 0.4 mmol), prepared by the method of Steward et al.,[17] was dissolved in hot benzene (25 mL) and poured into the Büchner funnel. The solution developed the characteristic green color of $Cu(O_2CCPh_3)_2\cdot py$ at this time. The height of the outer solution was then adjusted to ca. 1 cm above the level of the inner solution. The entire apparatus was placed in a desiccator. After four days, blue-green crystals of **1** had formed on the fritted disk in the filter. Anal. Calcd for $C_{48}H_{38}O_4CuN$: C, 76.22; H, 5.06; Cu, 8.40; N, 1.85%. Found: C, 76.15; H, 5.00; Cu, 8.45; N, 1.88%.

(b) $Cu(O_2CCPh_3)_2\cdot py$ (2a): Procedure 1. $Cu(O_2CCPh_3)_2\cdot 2H_2O$ (1.29 g, 1.91 mmol) was dissolved in benzene (150 mL). Warming on the steam bath reduces the time required for the complex to dissolve. Pyridine (0.59 g, 7.46 mmol) was added, resulting in a color change from blue to green. After filtering, the complex was precipitated by adding petroleum ether, bp 30—60 °C (700 mL). The light-green precipitate was collected in a Büchner funnel with a fritted disk (reduced-pressure filtration). The precipitate was washed with a benzene–petroleum ether mixture (1 : 9 v/v, 100 mL) and allowed to dry in air for several days, yielding 1.16 g, 1.62 mmol, (84.8% yield) of **2a**. Anal. Calcd for $C_{45}H_{35}O_4CuN$: C, 75.35; H, 4.92; Cu, 8.86; N, 1.95%. Found: C, 75.46; H, 5.00; Cu, 8.94 (EDTA titration), 8.52 (atomic absorption); N, 1.86%.[18]

Procedure 2. A mixture of $Cu(O_2CCPh_3)_2\cdot 2H_2O$ (0.67 g, 1.0 mmol) and pyridine (87 mg, 1.1 mmol) in chloroform (60 mL) was stirred on a hot plate for 0.5 h. The chloroform solution was then filtered, and the filtrate was concentrated to one-third of its volume. After standing overnight at ca. 5 °C, the concentrated solution afforded yellow-green crystals of **2a**. The crystals were washed with petroleum ether and dried in vacuo. Anal. Calcd for $C_{45}H_{35}O_4CuN$: C, 75.35; H, 4.92; Cu, 8.86; N, 1.95%. Found: C, 75.15; H, 4.65; Cu, 8.59; N, 2.12%.

(c) $Cu(O_2CCPh_3)_2\cdot py$ (2b). A mixture of $Cu(O_2CCPh_3)_2\cdot 2H_2O$ (0.67 g, 1.0 mmol) and pyridine (0.12 g, 1.5 mmol) in ethanol (50 mL) was heated with stirring on a hot plate for ca. 2 h. The resulting yellow-green precipitate was collected, washed repeatedly with ethanol and dried in vacuo. Anal. Calcd for $C_{45}H_{35}O_4CuN$: C, 75.35; H, 4.92; Cu, 8.86; N, 1.95%. Found: C, 74.62; H, 4.92; Cu, 9.11; N, 1.84%.

(d) $Cu(O_2CCPh_3)_2\cdot 2py$ (3), Crystals. Crystals of **1** were placed in a screw-capped vial containing an absolute ethanol–pyridine (50 : 1 v/v) solution. After one day, mixed crystals containing both blue-green and dark blue areas had formed. After three days, the blue-green crystals had been completely transformed into dark-blue crystals of **3**. Anal. Calcd for $C_{50}H_{40}O_4CuN_2$: C, 75.42; H, 5.06; Cu, 7.97; N, 3.51%. Found: C, 75.28; H, 4.99; Cu, 8.08; N, 3.50%.

Preparation of Triphenylacetic Acid-*d*. A small amount of triphenylacetic acid was dissolved with warming in ethanol-*d* (99.5+ atom % D). The solvent was removed by evaporation under a stream of dry nitrogen. The resulting solid was dried in a desiccator under reduced pressure.

X-Ray Procedure. (a) Collection and Reduction of the Data. The crystal of **1** selected was mounted on a glass fiber and coated with an epoxy resin. A crystal of **3** having the dimensions 0.15×0.19×0.32 mm was similarly mounted. Refined cell constants were obtained by a least-squares fit to the observed 2θ angles of 110 high-angle reflections. Data concerning the crystals are given in Table 1. The intensity data were collected using a Picker FACS-1 four-circle diffractometer to a 2θ limit of 90° for **1** and 125° for **3** using graphite-monochromated Cu $K\alpha$ radiation; a $\theta : 2\theta$ scanning technique over the range 2.5° for **1** and 2.2° for **3**; a scan rate of $1°\ \text{min}^{-1}$ was used. The background was counted for 20 s at each end of the scan range. For **1**, three standard reflections were monitored after each 100 reflections; their intensities decreased by ca. 9%. For **3**, three standard reflections were monitored after each 50 reflections; their intensities showed no fluctuations greater than ±2%. The intensities for **1** were scaled and assigned variances, $\sigma^2(\mathrm{I})$, according to the statistics of the scan and background counts plus the correctional term, $(0.03\ \mathrm{S})^2$, S being the scan count. The intensities and their variance were corrected for both Lorentz and polarization factors. For **3**, corrections were made for both absorbance and secondary extinction.[19]

Table 1. Crystallographic Data for $[Cu_2(O_2CCPh_3)_4(py)_2]\cdot C_6H_6$ (1) and $Cu(O_2CCPh_3)_2\cdot 2py$ (3)

	1	**3**
Formula	$C_{96}H_{76}Cu_2N_2O_8$	$C_{50}H_{40}CuN_2O_4$
Fw	1512.76	796.42
Space group	$P\bar{1}$	$P2_1/c$
$a/\text{Å}$	19.558(7)	8.931(1)
$b/\text{Å}$	16.605(6)	12.602(1)
$c/\text{Å}$	14.997(5)	19.578(1)
α/deg	114.55(2)	
β/deg	97.11(2)	118.17(0.4)
γ/deg	111.65(2)	
$V/\text{Å}^3$	3890.2	1942.5
$\lambda/\text{Å}$	1.54178	1.54178
Z	2	2
$\rho_c/\text{g cm}^{-3}$	1.297	1.401
μ/cm^{-1}	19.89	20.40
No. of unique data	6522	3107
No. of data with $I\geq 3\sigma(I)$	5599	2771
R	0.045	0.030
R_w	0.055	0.026

Solution and Refinement of the Structures. (a) $[Cu_2(O_2CCPh_3)_4(py)_2]\cdot C_6H_6$ (1). The triclinic unit cell was first determined from Weissenberg photographs and the $P\bar{1}$ space group was confirmed by the subsequent structure solution and refinement. The phase problem was solved by direct methods using the MULTAN program.[20] Two copper and 34 non-hydrogen atoms were located from the most probable E map. The corresponding Cu–Cu vectors were confirmed on an E^2-1 Patterson synthesis. After two difference Fourier syntheses, 102 atoms had been located. The 102 atom model, assumed to be complete, was subjected to full-matrix least-squares refinement using a program called QWKREF.[21] On the difference Fourier map, the benzene of solvation was revealed. Two more difference Fourier syntheses revealed all 71 hydrogen atoms bonded to the molecule. The hydrogen positions for the solvent ring were generated by a program called GENATM.[22] The atomic positional parameters and isotropic thermal parameters for hydrogen (3.7 Å) were included in the structure factor calculations, but were not refined. Four more cycles of refinement with anisotropic thermal parameters for all of the nonhydrogen atoms converged to R=0.045. The atomic scattering factors (Cu, C,·N, and O) and the anomalous dispersion corrections (Cu and O) were taken from Ref. 23a. The scattering factors for hydrogen were taken from Stewart et al.[23b)] The observed and calculated structure factors are included in the supplementary material.[24)]

(b) $Cu(O_2CCPh_3)_2 \cdot 2py$ (3). The structure was solved by the multi-solution tangent-refinement method.[20)] The best E map with 350 reflections (E>1.45) and 5000 phase relationships gave all of the nonhydrogen atom positions. The copper atom was located and the position confirmed by an origin removed Patterson synthesis. The positional parameters and isotropic thermal parameters of the nonhydrogen atoms were refined by several cycles of full-matrix least-squares using QWKREF program,[21)] yielding R=0.115. After conversion to anisotropic thermal paramters, several further cycles reduced R to 0.069. At this point, the hydrogen atoms were located and included in the refinement. After changing the weighting scheme from counting statistics to a scheme based on an analysis of the variance,[25)] the extinction correction was applied. Further refinement with the new weights converged to R=0.030. The atomic-scattering factors and anomalous-dispersion corrections employed are the same as those described in part (a). The observed and calculated structure factors are included in the supplementary material.[24)]

Physical Measurements. IR spectra were recorded on a Perkin-Elmer 1430 ratio recording spectrophotometer, polystyrene standard. Reflectance spectra were obtained on a Hitachi recording spectrophotometer (323). ESR spectra were obtained from polycrystalline samples in quartz tubes, DPPH standard, as described previously,[17)] except for samples of **2a**[26)] and **2b**.[27)]

Magnetic moments were determined in solution by the Evans method, as described previously.[17)] Magnetic susceptibilities over the temperature range of 80 to 300 K were determined by the Faraday method. Corrections for the diamagnetic contributions were made using Pascal's constants.[28)] The cryomagnetic data of complexes **1**, **2a**, and **2b** were fitted to the Bleaney-Bowers equation allowing for the presence of paramagnetic impurities,[29)]

$$\chi_A = \frac{Ng^2\beta^2}{3kT}\left[1+\left(\frac{1}{3}\right)\exp\left(\frac{-2J}{kT}\right)\right]^{-1}(1-P) + \frac{Ng_i^2\beta^2}{4kT}P + N\alpha, \tag{1}$$

where P is the mole fraction of the noncoupled copper(II) impurity and g_i is the average g factor for the impurity. The values of g_i=2.2 and $N\alpha = 60\times10^{-6}$ emu (1 cgs emu=$4\pi\times10^{-6}$ m^3) were used throughout this study. The other symbols have their usual meanings. The best-fit parameters ($-2J$, g, and P) were obtained by using a nonlinear least-squares program[30)] on a FACOM M-200 computer at the Nagoya University Computation Center. As a convenient statistical indicator of the quality of the least-squares fit, the discrepancy index, σ_{dis}, was employed,

$$\sigma_{dis} = \left[\frac{\sum(\chi_{obsd}-\chi_{calcd})^2}{\sum\chi_{obsd}^2}\right]^{1/2}. \tag{2}$$

The Curie law was employed to correlate the cryomagnetic data for **3** assuming no monomeric impurities and $N\alpha = 60\times10^{-6}$ emu.

Results and Discussion

Structures. Single-crystal X-ray structures have been determined for $[Cu_2(O_2CCPh_3)_4(py)_2]\cdot C_6H_6$ (**1**), Figs. 1a and 1b, and $Cu(O_2CCPh_3)_2\cdot 2py$ (**3**), Fig. 2. The atomic positional and isotropic thermal parameters for all atoms, except hydrogen, in the complexes are

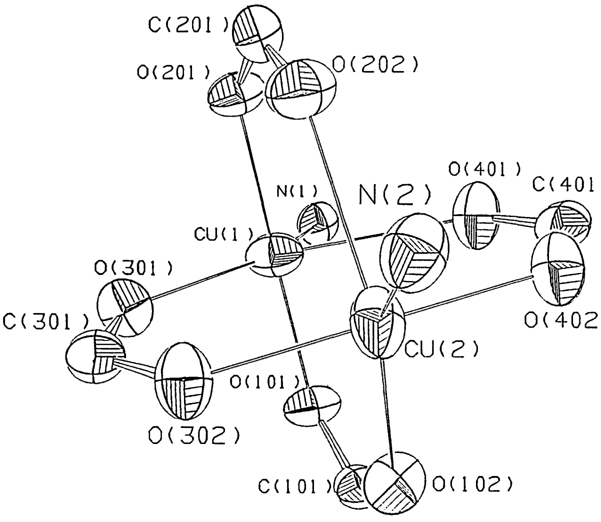

Fig. 1a. View of the cage structure of $[Cu_2(O_2CCPh_3)_4$-$(py)_2]\cdot C_6H_6$ (**1**). N(1) and N(2) are in py(P11) and py(P21) respectively. Thermal ellipsoids are drawn to the 50% probability level.

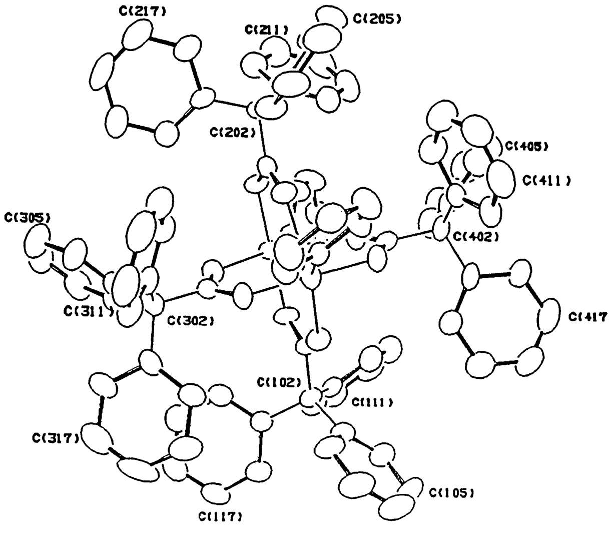

Fig. 1b. View of the structure of $[Cu_2(O_2CCPh_3)_4$-$(py)_2]\cdot C_6H_6$ (**1**). The orientation of the cage is the same as that shown in Figure 1a. For clarity, only a few atoms in the triphenylmethyl groups have been numbered, and the hydrogen atoms and the benzene of crystallization are omitted. Thermal ellipsoids are drawn to the 50% probability level.

listed in Tables 2 and 3; listings of the positional parameters for the hydrogen atoms are included in the supplementary material (Tables 1S and 7S). Selected bond distances and bond angles are given in Tables 4 and 5; complete tables are included in the supplementary material (Tables 3S and 9S).

The structure of **1** contains two crystallographically independent copper atoms and is novel in that the five atoms in the coordination sphere around copper(II) are arranged near neither the corners of a square pyramid nor the corners of a trigonal bipyramid. Each copper atom is coplanar with two oxygen atoms and a nitrogen

Table 2. Positional Parameters ($\times 10^4$) and Equivalent Isotropic Thermal Parameters (Å$^2\times 10$) and Their Standard Deviations for $[\mathrm{Cu_2(O_2CCPh_3)_4(py)_2}]\cdot\mathrm{C_6H_6}$ (**1**)

Atom	*x*	*y*	*z*	B_{eq} a)	Atom	*x*	*y*	*z*	B_{eq} a)
Cu(1)	1561(0)	9646(0)	9873(0)	30(0)	C(303)	1609(3)	8141(3)	11985(4)	27(2)
Cu(2)	3155(0)	9694(0)	9884(0)	30(0)	C(304)	1778(3)	8486(4)	13024(4)	43(3)
O(101)	1216(2)	8441(2)	8592(2)	30(1)	C(305)	1187(4)	8389(5)	13484(4)	56(3)
O(102)	2352(2)	8448(2)	8505(2)	30(1)	C(306)	428(4)	7937(4)	12879(6)	51(3)
O(201)	1941(2)	10854(2)	11162(2)	29(1)	C(307)	247(3)	7594(4)	11846(5)	44(3)
O(202)	3142(2)	11030(2)	11288(2)	34(2)	C(308)	831(3)	7684(3)	11387(4)	35(3)
O(301)	1734(2)	8940(2)	10655(2)	29(2)	C(309)	3062(3)	8727(4)	12257(3)	29(3)
O(302)	2862(2)	8915(2)	10542(2)	30(1)	C(310)	3463(3)	8226(4)	12397(4)	39(3)
O(401)	2323(2)	10572(2)	9116(2)	38(2)	C(311)	4220(4)	8793(6)	13132(5)	52(4)
O(402)	3425(2)	10449(2)	9215(2)	30(2)	C(312)	4563(3)	9812(6)	13695(4)	51(4)
N(P11)	726(2)	9918(3)	9265(3)	26(2)	C(313)	4161(3)	10303(4)	13560(4)	47(3)
N(P21)	4310(2)	10342(3)	10742(3)	25(2)	C(314)	3405(3)	9761(4)	12845(4)	36(3)
C(101)	1627(3)	8073(3)	8160(3)	26(2)	C(315)	2046(3)	7067(3)	10699(4)	31(3)
C(102)	1137(2)	7043(3)	7118(3)	27(2)	C(316)	1698(4)	6335(4)	10954(5)	59(3)
C(103)	1664(3)	6735(3)	6516(4)	31(2)	C(317)	1543(4)	5355(5)	10326(7)	77(4)
C(104)	1546(3)	6506(4)	5489(4)	42(3)	C(318)	1735(4)	5093(4)	9439(6)	72(4)
C(105)	1992(4)	6122(4)	4935(4)	57(3)	C(319)	2076(4)	5795(5)	9172(4)	58(3)
C(106)	2536(4)	5968(4)	5406(6)	59(3)	C(320)	2233(3)	6774(4)	9792(4)	42(3)
C(107)	2662(3)	6192(4)	6414(5)	52(3)	C(401)	2961(3)	10747(3)	8961(3)	29(2)
C(108)	2232(3)	6569(4)	6971(4)	41(3)	C(402)	3262(3)	11362(3)	8406(3)	29(2)
C(109)	567(3)	7203(4)	6486(3)	28(2)	C(403)	2746(3)	11836(4)	8239(4)	36(3)
C(110)	−223(3)	6548(3)	6034(4)	34(2)	C(404)	3070(3)	12819(4)	8454(4)	50(3)
C(111)	−718(3)	6731(4)	5473(4)	45(3)	C(405)	2577(5)	13181(5)	8183(5)	67(4)
C(112)	−435(4)	7553(5)	5349(4)	51(3)	C(406)	1788(5)	12580(6)	7719(5)	65(4)
C(113)	369(4)	8223(4)	5800(4)	50(3)	C(407)	1475(3)	11622(5)	7512(5)	58(4)
C(114)	849(3)	8035(4)	6356(4)	39(3)	C(408)	1939(3)	11228(4)	7745(4)	46(3)
C(115)	692(2)	6214(3)	7356(4)	27(2)	C(409)	4108(3)	12149(3)	9122(4)	32(3)
C(116)	491(3)	5227(4)	6663(4)	39(3)	C(410)	4759(3)	12129(4)	8843(4)	41(3)
C(117)	83(3)	4466(4)	6851(4)	47(3)	C(411)	5505(3)	12831(5)	9566(6)	56(4)
C(118)	−132(3)	4660(4)	7719(5)	47(3)	C(412)	5608(4)	13533(5)	10534(5)	61(3)
C(119)	53(3)	5627(5)	8411(4)	51(3)	C(413)	4967(4)	13550(5)	10818(4)	64(4)
C(120)	461(3)	6403(3)	8238(4)	41(3)	C(414)	4229(3)	12856(4)	10110(5)	51(3)
C(201)	2675(3)	11333(3)	11606(3)	28(3)	C(415)	3235(3)	10646(4)	7326(3)	28(3)
C(202)	2963(3)	12370(3)	12605(3)	27(2)	C(416)	3454(3)	11041(4)	6687(4)	45(3)
C(203)	3856(3)	13011(4)	12979(3)	30(2)	C(417)	3466(3)	10429(6)	5709(5)	57(4)
C(204)	4197(3)	14012(4)	13233(4)	41(3)	C(418)	3276(3)	9452(5)	5372(4)	47(3)
C(205)	5019(4)	14580(4)	13655(4)	49(3)	C(419)	3039(3)	9048(4)	5986(4)	43(3)
C(206)	5480(3)	14162(5)	13794(4)	52(3)	C(420)	3015(3)	9650(4)	6960(4)	34(3)
C(207)	5138(3)	13178(4)	13540(4)	47(3)	C(P11)	150(3)	9221(4)	8366(4)	39(3)
C(208)	4336(3)	12599(4)	13144(4)	41(3)	C(P12)	−382(3)	9427(4)	7929(4)	44(3)
C(209)	2526(3)	12863(3)	12284(4)	30(2)	C(P13)	−341(3)	10346(4)	8406(4)	42(3)
C(210)	2010(3)	13111(4)	12744(4)	45(3)	C(P14)	242(3)	11054(4)	9338(4)	45(3)
C(211)	1600(4)	13501(5)	12367(6)	63(4)	C(P15)	770(3)	10825(4)	9740(4)	37(3)
C(212)	1684(4)	13626(4)	11536(6)	63(4)	C(P21)	4568(3)	9957(4)	11236(4)	37(3)
C(213)	2198(4)	13366(4)	11064(4)	53(3)	C(P22)	5337(3)	10389(4)	11826(4)	44(3)
C(214)	2609(3)	12988(4)	11433(4)	39(3)	C(P23)	5867(3)	11251(4)	11911(4)	38(3)
C(215)	2769(3)	12208(4)	13501(3)	31(2)	C(P24)	5610(3)	11650(4)	11402(4)	44(3)
C(216)	3049(3)	13046(4)	14481(4)	55(3)	C(P25)	4822(3)	11190(4)	10830(4)	42(3)
C(217)	2894(4)	12958(5)	15317(4)	67(4)	C(BZ1)	4999(8)	3548(14)	7115(23)	130(9)
C(218)	2454(4)	12026(6)	15188(5)	60(4)	C(BZ2)	5105(14)	3182(10)	6199(17)	150(10)
C(219)	2172(3)	11183(4)	14225(5)	50(3)	C(BZ3)	5832(19)	3319(15)	6230(17)	150(13)
C(220)	2328(3)	11282(4)	13392(4)	34(3)	C(BZ4)	6368(9)	3788(16)	7090(26)	184(15)
C(301)	2263(3)	8718(3)	10828(3)	26(2)	C(BZ5)	6291(16)	4123(14)	8014(17)	211(13)
C(302)	2232(2)	8153(3)	11451(3)	25(2)	C(BZ6)	5561(18)	4013(12)	7955(12)	156(11)

a) B_{eq} equals one-third of the trace of the orthogonalized B_{ij} matrix.

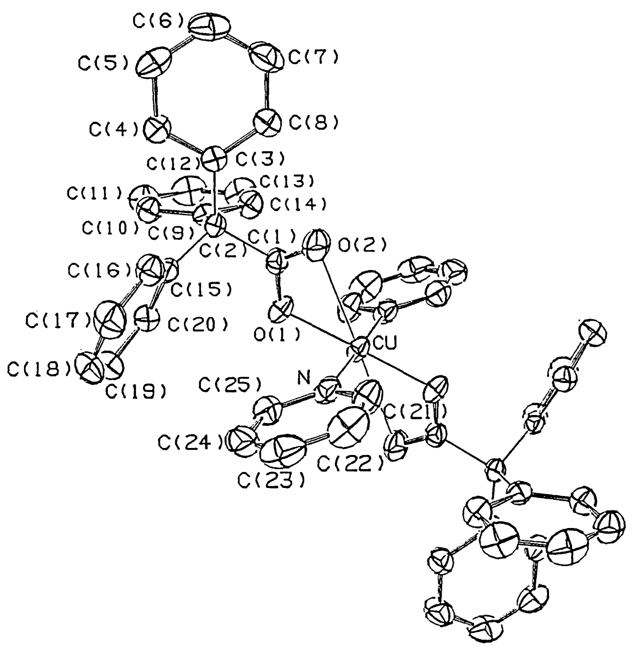

Fig. 2. View of the molecular structure of Cu(O_2CCPh_3)$_2$·2py (**3**). For clarity, the hydrogen atoms are omitted. Thermal ellipsoids are drawn to the 50% probability level.

Table 3. Positional Parameters (×10^4) and Equivalent Isotropic Thermal Parameters (Å^2×10) and Their Standard Deviations for Cu(O_2CCPh_3)$_2$·2py (**3**)

Atom	x	y	z	B_{eq}[a)]
Cu	0(0)	5000(0)	5000(0)	25(0)
O(1)	514(2)	6393(1)	5509(1)	28(0)
O(2)	−234(2)	5510(1)	6271(1)	44(1)
N	−2517(2)	5281(1)	4507(1)	29(1)
C(1)	266(2)	6319(2)	6102(1)	25(1)
C(2)	535(2)	7379(1)	6567(1)	20(1)
C(3)	527(2)	7220(2)	7348(1)	23(1)
C(4)	39(3)	8036(2)	7674(1)	29(1)
C(5)	132(3)	7930(2)	8400(1)	39(1)
C(6)	731(3)	7013(2)	8814(2)	43(1)
C(7)	1269(3)	6203(2)	8515(1)	43(1)
C(8)	1175(3)	6304(2)	7787(1)	33(1)
C(9)	2283(2)	7871(2)	6781(1)	22(1)
C(10)	2540(3)	8960(2)	6867(1)	29(1)
C(11)	4142(3)	9391(2)	7090(1)	38(1)
C(12)	5501(3)	8738(2)	7251(2)	43(1)
C(13)	5278(3)	7660(2)	7192(1)	40(1)
C(14)	3679(3)	7225(2)	6957(1)	30(1)
C(15)	−950(2)	8056(2)	5979(1)	23(1)
C(16)	−2549(3)	8010(2)	5943(1)	30(1)
C(17)	−3934(3)	8519(2)	5348(2)	42(1)
C(18)	−3762(3)	9073(2)	4788(2)	45(1)
C(19)	−2201(3)	9122(2)	4811(1)	39(1)
C(20)	−815(3)	8617(2)	5401(1)	29(1)
C(21)	−3574(3)	4479(2)	4434(1)	37(1)
C(22)	−5299(3)	4620(3)	4128(2)	47(1)
C(23)	−5982(3)	5594(3)	3874(2)	49(1)
C(24)	−4934(4)	6421(3)	3946(1)	47(1)
C(25)	−3196(3)	6242(2)	4269(1)	37(1)

a) B_{eq} equals one-third of the trace of the orthogonalized B_{ij} matrix.

atom: Cu(1), O(301), O(401), N(1) and Cu(2), O(102), O(202), N(2).[31)] The O–Cu–X angles, where X is N or O, between coplanar atoms for Cu(1) and Cu(2) are 82°, 136°, 142° and 84°, 136°, 139° respectively. There are six O–Cu–X angles for each copper in the range 88—92° and one large O–Cu–O angle between 178—179°. The Cu–O bond distances for each copper vary over a considerable range, Cu(1) 1.90—2.46 Å and Cu(2) 1.88—2.35 Å.[32)] The out-of-plane Cu–O bonds are very short, Cu(1) 1.90—1.91 Å and Cu(2) 1.88—1.90 Å respectively. One in-plane Cu–O bond to each copper is unusually long, 2.46 and 2.35 Å for Cu(1) and Cu(2) respectively. These Cu–O bonds are the longest that have been observed for a bridging carboxylato ligand in a dimeric copper(II) complex.[5)] The Cu–N bonds are somewhat shorter than those previously observed for apical ligands in dimeric copper(II) carboxylates.

In **1**, where the ligands bonded to copper(II) do not assume a configuration which coincides with or is closely related to one of the usual five-coordinate geometries, square pyramidal or trigonal bipyramidal, one cannot readily decide by inspection whether to describe the arrangement of the ligands as distorted square pyramidal or distorted trigonal bipyramidal. Zemann[33)] has described a test which allows one to make a rational choice between these two alternatives by considering the sum of the deviations of the angles between the ligands and the central metal atom in the complex from the angles in the idealized structures. Based on this test, the arrangement of the ligands in **1** is best described as distorted trigonal bipyramidal.

The cage structure of **1** is very unusual as a result of the ligand arrangement around each copper(II). The structure of the cage is depicted in Fig. 1a. The two distorted trigonal bipyramids formed by the ligands around each copper(II) are linked through the four bridging carboxylato ligands, spanning the apical and equatorial positions, to form a cage in which the dihedral angle between the equatorial planes is 88.8°. There are two adjacent short and long bridge distances in the cage: 6.48, 6.49, 6.78, and 6.86 Å. While the two short bridge distances are in the range reported for the complexes with copper(II) acetate monohydrate-type structures,[3,4)] the distances of the other two bridges are the longest observed to date. The long bridge distances are primarily the result of the long Cu–O bonds, one to each copper(II). A considerable variation in the Cu–O–C angles is observed, 116—140°, with the two largest angles encompassing the long Cu–O bonds. However, there is no corresponding opening of the O–C–O angle; the mean value is 125°. As a result of the two long bridge distances, the Cu–Cu distance (3.086 Å) across the cage is much longer than that encountered in complexes where the four carboxylate bridges are of approximately the same length.[5)]

The spatial relationships between the two pyridine rings which lie within the molecule, py(P11) and py(P21), and the corresponding two pyridine rings in

Table 4. Selected Bond Distances (Å) and Angles (deg) for $[Cu_2(O_2CCPh_3)_4(py)_2]\cdot C_6H_6$ (**1**)

	Distances		
Cu(1)-Cu(2)	3.086(1)	O(101)-C(101)	1.264(5)
Cu(1)-O(101)	1.907(3)	O(102)-C(101)	1.252(5)
Cu(1)-O(201)	1.905(3)	O(201)-C(201)	1.271(5)
Cu(1)-O(301)	2.049(3)	O(202)-C(201)	1.251(5)
Cu(1)-O(401)	2.458(3)	O(301)-C(301)	1.252(5)
Cu(1)-N(1)	2.053(4)	O(302)-C(301)	1.272(5)
Cu(2)-O(102)	2.065(3)	O(401)-C(401)	1.248(5)
Cu(2)-O(202)	2.349(3)	O(402)-C(401)	1.271(5)
Cu(2)-O(302)	1.903(3)	C(101)-C(102)	1.576(6)
Cu(2)-O(402)	1.883(3)	C(201)-C(202)	1.567(6)
Cu(2)-N(2)	2.062(4)	C(301)-C(302)	1.568(6)
		C(401)-C(402)	1.569(6)
	Angles		
O(101)-Cu(1)-O(201)	178.0(1)	Cu(1)-O(101)-C(101)	127.7(4)
O(101)-Cu(1)-O(301)	89.3(1)	Cu(1)-O(201)-C(201)	116.2(4)
O(101)-Cu(1)-O(401)	88.5(1)	Cu(1)-O(301)-C(301)	132.3(3)
O(101)-Cu(1)-N(1)	90.1(1)	Cu(1)-O(401)-C(401)	136.1(4)
O(201)-Cu(1)-O(301)	89.9(1)	Cu(2)-O(102)-C(101)	131.1(4)
O(201)-Cu(1)-O(401)	90.8(1)	Cu(2)-O(202)-C(201)	140.1(4)
O(201)-Cu(1)-N(1)	91.6(1)	Cu(2)-O(302)-C(301)	126.1(3)
O(301)-Cu(1)-O(401)	136.3(1)	Cu(2)-O(402)-C(401)	119.1(3)
O(301)-Cu(1)-N(1)	141.7(1)	O(101)-C(101)-O(102)	125.6(4)
O(401)-Cu(1)-N(1)	82.0(1)	O(101)-C(101)-C(102)	113.7(4)
O(102)-Cu(2)-O(202)	136.4(1)	O(102)-C(101)-C(102)	120.7(4)
O(102)-Cu(2)-O(302)	88.0(1)	O(201)-C(201)-O(202)	124.4(4)
O(102)-Cu(2)-O(402)	91.0(1)	O(201)-C(201)-C(202)	114.1(4)
O(102)-Cu(2)-N(2)	139.3(1)	O(202)-C(201)-C(202)	121.5(4)
O(202)-Cu(2)-O(302)	89.4(1)	O(301)-C(301)-O(302)	125.7(4)
O(202)-Cu(2)-O(402)	90.9(1)	O(301)-C(301)-C(302)	120.7(4)
O(202)-Cu(2)-N(2)	84.2(1)	O(302)-C(301)-C(302)	113.6(4)
O(302)-Cu(2)-O(402)	178.8(1)	O(401)-C(401)-O(402)	124.7(4)
O(302)-Cu(2)-N(2)	90.8(1)	O(401)-C(401)-C(402)	122.0(5)
O(402)-Cu(2)-N(2)	90.4(1)	O(402)-C(401)-C(402)	113.3(4)

Table 5. Selected Bond Distances (Å) and Angles (deg) for $Cu(O_2CCPh_3)_2\cdot 2py$ (**3**)

	Distances		
Cu-O(1)	1.964(1)	C(1)-C(2)	1.570(3)
Cu-O(2)	2.673(2)	C(2)-C(3)	1.545(3)
Cu-N	2.015(2)	C(2)-C(9)	1.543(3)
O(1)-C(1)	1.284(2)	C(2)-C(15)	1.540(3)
O(2)-C(1)	1.220(2)		
	Angles		
N-Cu-O(1)	91.51(6)	O(1)-C(1)-O(2)	123.2(2)
N-Cu-O(2)	80.99(6)	O(1)-C(1)-C(2)	114.7(2)
O(1)-Cu-O(2)	54.15(6)	O(2)-C(1)-C(2)	122.0(2)
Cu-O(1)-C(1)	107.2(1)		

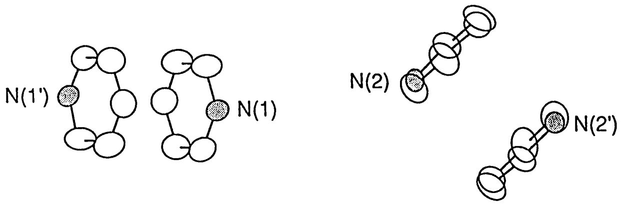

Fig. 3. View of the two intramolecular pyridine rings, py(P11) and py(P21), and the adjacent intermolecular pyridine rings, py(P11′) and py(P21′), along the *a* crystal axis of $[Cu_2(O_2CCPh_3)_4(py)_2]\cdot C_6H_6$ (**1**). N(1), (N1′), N(2), and N(2′) are in py(P11), py(P11′), py(P21), and py(P21′) respectively.

adjacent molecules, py(P11′) and py(P21′), along the *a* crystal axis, are shown in Fig. 3. The two intramolecular pyridine rings are tilted with respect to the Cu-Cu axes [Cu(2)-Cu(1)-N(1), 144.5°; Cu(1)-Cu(2)-N(2), 146.3°] toward the long Cu-O bonds, and the dihedral angles between the planes of the pyridine rings and the planes of the long bridging carboxyl groups are: py(P11)-carboxyl[O(401)C(401)O(402)], 81° and py(P21)-carboxyl[O(202)C(201)O(201)], 72°. The dihedral angle between the pyridine rings is 49.1°. The pyridine rings on adjacent molecules abut these rings resulting in parallel alignments (required by symmetry), as shown in Fig. 3. The intermolecular distances between the least-squares planes of the two intramolecular pyridine rings and the atoms of the adjacent rings are given in Table 6.

The conformations of the triphenylacetato ligands are of interest since intergroup repulsions could, in part, account for the unusual geometry around copper(II). The $C-CO_2^-$ bond lengths (mean of 1.570 Å) are unusually long for an sp^3-sp^2 C-C bond. The triphenylmethyl groups C(101)-C(120) and C(301)-C(320) have left-

Table 6. Intermolecular Distances between the Least-Squares Planes of the Two Intramolecular Pyridine Rings, py(P11) and py(P21) and the Atoms of the Adjacent Pyridine Rings, py(P11′) and py(P21′), along the *a* Crystal Axis in $[Cu_2(O_2CCPh_3)_4(py)_2] \cdot C_6H_6$ (**1**)[a,b]

py(P11)–py(P11′)		py(P21)–py(P21′)	
Atom	Distance (Å)	Atom	Distance (Å)
N(1′)	3.418	N(2′)	3.471
C(P11′)	3.409	C(P21′)	3.471
C(P12′)	3.417	C(P22′)	3.478
C(P13′)	3.422	C(P23′)	3.476
C(P14′)	3.405	C(P24′)	3.466
C(P15′)	3.421	C(P25′)	3.483

a) The prime designates the adjacent pyridine ring.
b) py(P11)–py(P21), dihedral angle, 49.1°.

handed twist propeller conformations while the twists for the groups C(201)–C(220) and C(401)–C(420) are right-handed. Jeffery et al.[34] has reported the simultaneous occurrence of two conformations in one molecule in bis(triphenylmethyl) sulfide. The angles between the phenyl rings exhibit a better threefold symmetry in the left-handed conformations than in the right-handed ones. All of the phenyl rings are coplanar with a maximum deviation of 0.142 Å. The torsion angles for defining these groups are given in Table 5S. The intramolecular distances between the ligands in **1** of < 3.7 Å are listed in Table 6S.

The benzene of crystallization is held in the crystal structure by van der Waals interactions and is lost when the crystal is allowed to stand in an open container. The ring shows considerable thermal motion.

The structure of the complex, $[Cu_2(O_2CCPh_3)_4(py)_2]$, can vary, depending on the method of preparation (see Experimental Section). The crystal structures of the two forms of $[Cu_2(O_2CCPh_3)_4(py)_2]$ (**2a**, **2b**) have not been determined; however, some conclusions concerning their molecular structures can be formulated based on their magnetic and spectral properties, vide infra. The molecular structures of **2a** and **1** must be closely related since both complexes give similar magnetic and spectral data; therefore, **2a** is assigned a distorted trigonal bipyramidal structure similar to that of **1**. The method of preparation of **2a** (Procedure 1 or 2) may result in small structural differences. The molecular structure of **2b** is more closely akin to the classical copper(II) acetate monohydrate-type structure. The magnetic and spectral data observed for **2b** are in agreement with this assignment.

The structure of $Cu(O_2CCPh_3)_2 \cdot 2py$ (**3**), Fig. 2, is a variation of the *trans*-bis(acetato-*O,O′*)diamminecopper(II) type.[35] In this structure, the two triphenylacetato and two pyridine ligands are bonded to copper(II); the copper(II) lies at a center of symmetry. The coordination plane around copper(II) consists of two triphenylacetate oxygen atoms, O(1) and O′(1) and two nitrogen atoms N and N′ in a nearly square planar arrangement. The second carboxyl oxygens, O(2) and O(2′), are weakly bonded to copper(II) above and below the plane: the weak Cu–O bond distance is 2.673 Å, the O(1)–Cu–O(2) angle is 54.1°, and the N–Cu–O(2) angle is 81.0°. The dihedral angle between the coordination plane around copper(II) and the plane of the carboxyl group is 78.0°. The coordination geometry around copper(II) is best described as distorted octahedral.

In the triphenylacetato ligands, the carboxyl O(1)–C(1)–O(2) angle is 123.2°. The C–O bond lengths are significantly different: C(1)–O(1), 1.284 Å and C(1)–O(2), 1.220 Å, which suggests that the shorter C–O bond has considerably more double-bond character. The dihedral angle between the plane of the pyridine ring and carboxyl group is 80.6°. As in **1**, the $C-CO_2^-$ bond length (1.570 Å) is unusually long for an sp^3–sp^2 C–C bond. The triphenylmethyl group has a non-propeller conformation and a pseudo bisector plane passing through the atoms, C(1), C(2), C(15), and C(18).

The molecules of **3** are packed only by van der Waals forces. A stereoscopic ORTEP packing diagram is included in the supplementary material (Fig. 1S) along with the following tables: least-squared planes (Table 10S), torsion angles (Table 11S), and intramolecular nonbonded distances <3.26 Å (Table 12S).

Magnetic Susceptibility. The magnetic susceptibility data of the dimeric complexes **1**, **2a**, and **2b** were correlated using Eq. 1 (see Fig. 4). The best-fit parame-

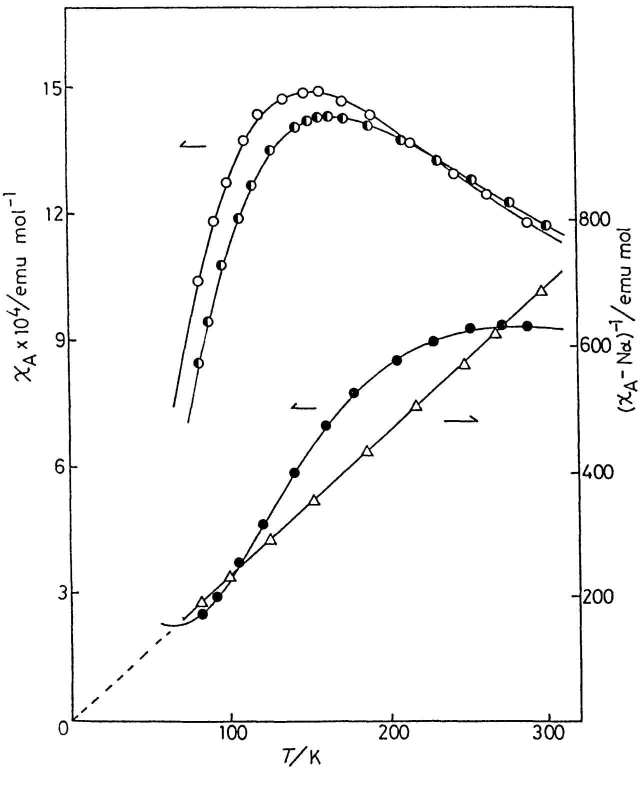

Fig. 4. Variation of the magnetic susceptibilities of the complexes with temperature: $[Cu_2(O_2CCPh_3)_4(py)_2] \cdot C_6H_6$ (**1**) (◐); $[Cu_2(O_2CCPh_3)_4(py)_2]$ (**2a**) (○), (**2b**) (●); $Cu(O_2CCPh_3)_2 \cdot 2py$ (**3**) (△).

ters are given in Table 7 along with the discrepancy index (Eq. 2). The $-2J$ values of complexes **1** and **2a** are considerably smaller than the values reported for a large number of copper(II) carboxylates with a square pyramidal metal geometry, ca. 300 cm^{-1}.[5] The anomalously small $-2J$ values observed for these dimeric complexes are undoubtedly related to the novel geometry around copper, distorted trigonal bipyramidal. The small singlet-triplet separation in these complexes may be interpreted in terms of their unusual cage structure. In a bridged structure similar to that observed for **1**, in which each copper has a distorted trigonal bipyramidal metal geometry, the two ends of a Cu–O–C–O–Cu exchange pathway would connect with different metal d orbitals: one end with the $d_{x^2-y^2}$, d_{xy} orbitals having paired electrons and the other with the d_{z^2} orbital having an unpaired electron.[36]. The copper(II) carboxylates with a square pyramidal metal geometry are known to have $-2J$ values of ca. 300 cm^{-1}, as observed for copper(II) acetate monohydrate, while theoretically, those with a regular trigonal bipyramidal metal geometry should have $-2J$ values close to zero (ferromagnetic). Thus, complexes **1** and **2a**, which have intermediate $-2J$ values, are expected to have a metal geometry in between a regular square pyramidal and a regular trigonal bipyramidal arrangement. The $-2J$ value determined for **2b** is consistent with a structure for this complex, which is closely related to the classical copper(II) acetate monohydrate type.

The magnetic behavior of **3** is consistent with the monomeric structure determined in the present study (see Figs. 2 and 4, Table 7).

Electron Spin Resonance. The X-band ESR spectra of polycrystalline samples of the $Cu(O_2CCPh_3)_2 \cdot n$py complexes have been recorded. The ESR data for these complexes at ambient temperature are given in Table 8.

Table 7. Magnetic Parameters for the $Cu(O_2CCPh_3)_2 \cdot n$ py Complexes, Faraday Method

Complex	$-2J$/cm^{-1}	$\bar{g}$	$P\times10^2$	$\sigma_{dis}\times10^3$
1	187	2.20	1.04	3.17
2a[a]	173	2.14	2.56	2.00
2b	321	2.29	2.10	5.51
3	—	2.15	—	4.53

a) Prepared by Procedure 2.

Table 8. ESR Parameters for Polycrystalline $Cu(O_2CCPh_3)_2 \cdot n$ py Complexes[a]

Complex	$g_\parallel$	$g_\perp$	$\bar{g}$	D/cm^{-1}
1[b]	2.26	2.06	2.13	0.198
2a[c,d]	2.25	2.06	2.13	0.201
2b[e]	2.38	2.07	2.18	0.366
3[f]	2.28	2.06	2.14	

a) Ambient temperature. b) H_{dq}=2777 G and H_m=3150 G at 9.06 GHz. c) Prepared by Procedure 1. d) H_{dq}=2910 G at 9.34 GHz. e) H_m=3300 G at 9.46 GHz; $A_\parallel$=0.0070 cm^{-1}. f) $A_\parallel$=0.0175 cm^{-1}.

The X-band ESR spectrum of **1** is different from the spectra reported for dimeric copper(II) carboxylates in which the metal geometry is square pyramidal. The difference arises as a result of the small zero-field splitting, D, in **1** which is less than the microwave energy ($h\nu$); whereas, $D>h\nu$ for dimeric copper(II) carboxylates with approximately square pyramidal geometry. The ESR spectrum of **1** at ambient temperature (9.05 GHz) is shown in Fig. 5. The spectrum consists of two $H_\parallel$ lines (927, 4790 G) and two $H_\perp$ lines (1780, 4050 G) as well as a line resulting from a double quantum transition (2780 G) and a weak line from a monomeric impurity (3150 G). The number and positions of the lines are consistent with theoretical calculations for randomly oriented molecules in the triplet state.[37] The isotropic double quantum absorption is observed when $1/2\ h\nu<D<h\nu$.[38] The ESR spectrum of **1** at 133 K is essentially the same as at ambient temperature, except for the relative intensities of the monomer and dimer lines. Since our initial report,[8] two other copper(II) carboxylates have been observed to have similar ESR spectra.[10,13]

The small zero-field splitting parameter (D) undoubtedly is the result of the novel geometry of **1**. This parameter consists of a dipolar term (D_{dip}) which is a function of the Cu–Cu distance, and a pseudo-dipolar term (D_{ex}) which results from an exchange coupling via the orbitals of the cage.[38,39] For **1**, the smaller D parameter can be related to the geometry of the cage in which the long Cu–Cu distance and the two very long bridging distances are contributing factors.

The ESR spectrum of **2a** at ambient temperature is similar to the spectrum of **1** with nearly identical ESR parameters. The spectral similarity between **1** and **2a** suggests that removing the benzene of crystallization from **1** has little effect on the dimer structure. These

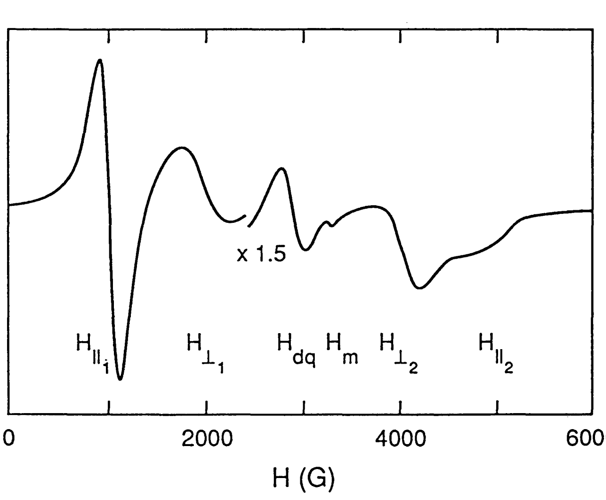

Fig. 5. The ESR spectrum (X-band, 9.05 GHz) of polycrystalline $[Cu_2(O_2CCPh_3)_4(py)_2] \cdot C_6H_6$ (**1**) at ambient temperature.

data suggest that the crystal structures of **1** and **2a** are similar, except for the benzene of crystallization.

The ESR spectrum of **2b** at 130 K shows three absorption lines which are typical of a dimeric copper(II) carboxylate when $D > h\nu$[3,4) and a line attributed to a monomer impurity. The hyperfine splitting of the low-field absorption line yields a seven-line pattern. The spectrum at ambient temperature is essentially the same, except that the hyperfine structure is not as well resolved. These data, along with the magnetic susceptibility data, suggest that the structure of **2b** is more closely aligned with the copper(II) acetate monohydrate-type structure than **1** and **2a**.

The ESR spectra of **3** at 133 K and ambient temperatures are quite typical of a monomeric copper(II) complex with a distorted octahedral geometry, showing two spectral lines resulting from the parallel and perpendicular alignments of the complex with the field;[40) the hyperfine coupling splits the low-field absorption, yielding a four-line pattern, of which only three are resolved.

Electronic Spectra. The reflectance spectra of the four copper(II) triphenylacetate-pyridine complexes are shown in Fig. 6, and the spectral data are reported in Table 9.

The most striking difference in the spectral features of the three dimeric complexes (**1**, **2a**, and **2b**) is the separation of the two peaks in the d–d band region. The peak separations in **1** and **2a**, which have a distorted trigonal bipyramidal metal geometry, are about 2000 cm^{-1}, while this separation in **2b** is 5000 cm^{-1}, a value observed for copper(II) carboxylates with the common square pyramidal geometry.[10,13) Thus, the electronic spectral data augments the proposal that complex **2b** has a structure which is closely aligned with the classical copper(II) acetate monohydrate type.

Table 9. Reflectance Spectral Data for the $Cu(O_2CCPh_3)_2 \cdot n$ py Complexes

Complex	$\tilde{\nu}_{max}\times10^{-3}$/cm^{-1}		$\Delta\tilde{\nu}\times10^{-3}$/cm^{-1}
1	13.68	11.75	1.93
2a[a)	13.51	11.49	2.02
2b	13.53	8.53	5.00
3	17.48	15.38	2.10

a) Prepared by Procedure 2.

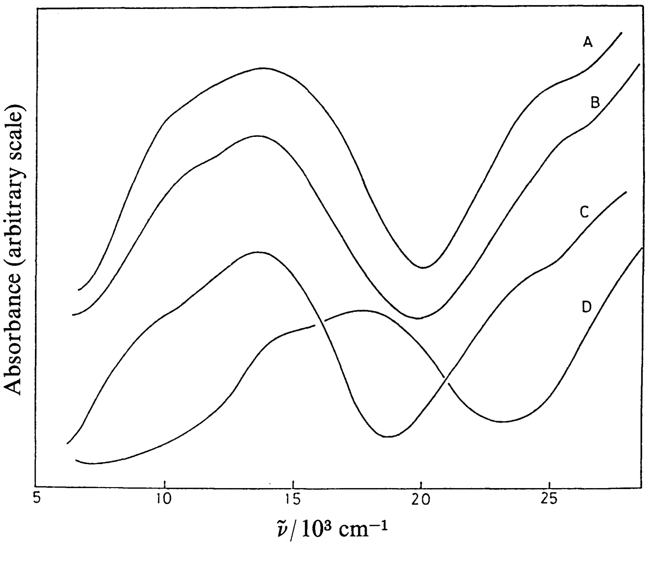

Fig. 6. Reflectance spectra of the complexes: $[Cu_2(O_2CCPh_3)_4(py)_2] \cdot C_6H_6$ (**1**) (A); $[Cu_2(O_2CCPh_3)_4(py)_2]$ (**2a**) (B); (**2b**) (C); $Cu(O_2CCPh_3)_2 \cdot 2py$ (**3**) (D).

Another salient feature of the electronic spectra of the dimeric complexes **1**, **2a**, and **2b** is that the d–d band energies are about the same, **1** and **2a** having only slightly higher band energies, in spite of the structural differences. This same type of behavior has been reported for the copper(II) trichloroacetate adducts.[10–13) The d–d band energy of copper(II) complexes with trigonal bipyramidal metal geometry is reported to be lower than the band energy of the corresponding complexes with square pyramidal metal geometry.[36) The anomalously high d–d band energy observed for complexes **1** and **2a** may be ascribed to the short Cu–O bonds in the axial coordination sites which raise the energy of the d_{z^2} orbital.

The d–d band of **3**, ca. 17×10^3 cm^{-1}, occurs at higher energy than that observed for **1**, **2a**, and **2b** (ca. 13×10^3 cm^{-1}), indicating that the ligand field in complex **3** is stronger than in the latter complexes. This shift to higher energy of the d–d band of **3** undoubtedly reflects the difference in the number of coordinating atoms and the metal geometry, distorted octahedral.[41)

The so-called "dimer band" is observed as a shoulder in the near-ultraviolet region for complexes **1**, **2a**, and **2b**. This band has been reported for a large number of dimeric copper(II) carboxylates and other dimeric copper(II) systems.[42–44) The spectrum of the monomeric complex **3** does not show an absorption band in this region.

Infrared Spectra. The carbon-oxygen stretching frequencies of the copper(II) triphenylacetate-pyridine complexes are given in Table 10. The splitting of the RCO_2^- stretching frequencies, $\Delta\tilde{\nu} = \tilde{\nu}_{asym} - \tilde{\nu}_{sym}$, is related to the symmetry of the carboxylato group: the greater the deviation from C_{2v} symmetry, the larger the $\Delta\tilde{\nu}$

Table 10. Carbon-Oxygen Stretchig Frequecies of the Triphenylacetato Ligand for the $Cu(O_2CCPh_3)_2 \cdot n$ py Complexes[a,b)

Complex	$\tilde{\nu}_{asym}$/cm^{-1}	$\tilde{\nu}_{sym}$/cm^{-1}	$\Delta\tilde{\nu}$/cm^{-1}
1	1639	1369	270
2a[c)	1638	1367	271
2b	1627	1371	256
3	1613	1320	293

a) KBr disk. b) The following stretching frequencies were obtained for the conjugate acid form of the ligand, Ph_3CCO_2H: (C=O) 1696, (C–O) 1271; Ph_3CCO_2D: (C=O) 1692, (C–O) 1300 cm^{-1}. c) Prepared by Procedure 1.

values.[45—47] The order observed for $\Delta\bar{\nu}$ for the copper(II) triphenylacetate-pyridine complexes is **3**>**1**, **2a**>**2b**. This is the order expected from symmetry considerations for the carboxylato ligands in these complexes based on the structural, magnetic, and spectral properties given above. The C–O bond distance data (Tables 4 and 5) for complexes **1** and **3** show that there is a greater difference in the C–O bond lengths in the carboxylato ligands in **3** than in **1**. In complex **2b**, which is proposed to have a structure more closely aligned with the copper(II) acetate monohydrate type than **1**, the bridging carboxylato groups are expected to be more symmetrical than in **1**, where there is a considerable variation in the C–O bond lengths in each bridging group.

Discussion of Structures. The first reports of dimeric copper(II) carboxylates with a distorted trigonal bipyramidal geometry around copper are for $[Cu_2(O_2CCPh_3)_4(py)_2]\cdot C_6H_6$ (**1**)[7,8] and $[Cu_2(O_2CCCl_3)_4(L)_2]$, where L=tempo and proxyl.[11,12] The main structural differences between **1** and the above-mentioned trichloroacetate complexes are: in **1**, the carboxylato bridging distances are longer and the equatorial angles show larger deviations from the ideal trigonal bipyramidal geometry. Thus, in **1**, there is considerably more distortion of the geometry around copper. Recently, preliminary reports of additional dimeric complexes with distorted trigonal bipyramidal metal geometry have appeared: $[Cu_2(O_2CCPh_3)_4(\gamma\text{-picoline})_2]\cdot$2toluene,[9] $[Cu_2(O_2CCPh_3)_4(\gamma\text{-picoline})_2]\cdot$2benzene,[9] $[Cu_2(O_2CCCl_3)_4(\text{caffeine})_2]$,[14,16] $[Cu_2(O_2CCCl_3)_4(2,5\text{-}Cl_2\text{-}py)_2]\cdot$benzene,[16] $[Cu_2(O_2CCCl_3)_4(3,5\text{-}Cl_2\text{-}py)_2]\cdot$toluene.[16]

The structural transformation of **1** from the usual square pyramidal arrangement of ligands around copper(II), as observed in the classical copper(II) acetate-type structure, to a distorted trigonal bipyramidal arrangement, can best be explained in terms of steric effects in the crystal environment which can arise from both inter- and intramolecular forces. The crystal-structure data for **1** suggest that crystal-packing forces play an important role in this transformation. Along the *a* crystal axis, the pyridine rings at the opposite ends of the molecule form a dihedral angle of 49.1°. The pyridine rings on adjacent molecules abut these rings resulting in a parallel alignment (cf. Fig. 3 and Table 6). The intermolecular distances between the pyridine rings and the atoms of the adjacent rings are ca. 3.41 Å for py(P11)–py(P11′) and 3.47 Å for py(P21)–py(P21′) respectively. These distances approach the value reported by Pauling[48] for the effective thickness of an aromatic ring, 3.4 Å. Cu(1) which shows the largest distortion from a square pyramidal structure, N(1)–Cu(1)–O(401), 82.0°; Cu(2)–Cu(1)–N(1), 144.50°; Cu(1)–O(401), 2.458 Å, is bonded to the py(P11) with the smallest intermolecular distance, while Cu(2) which is bonded to py(P21) shows less distortion, N(2)–Cu(2)–O(202), 84.2°; Cu(1)–Cu(2)–N(2), 146.3°; Cu(2)–O(202), 2.349 Å. These data indicate that crystal packing forces are an important factor in determining the geometry around copper(II).

The complex, $[Cu_2(O_2CCPh_3)_4(py)_2]$, exists in two crystalline modifications which exhibit different magnetic and spectral properties. Form **2a** was prepared by allowing **1** to lose the benzene of crystallization upon standing in an open container (Procedure 1) or by crystallizing the complex from a chloroform solution (Procedure 2). The magnetic and spectral properties of **2a** are nearly identical to those of **1**, suggesting that the crystal structures are similar with or without the benzene of crystallization. Form **2b** was prepared by crystallization of $[Cu_2(O_2CCPh_3)_4(py)_2]$ from an ethanol solution. The magnetic and spectral properties of **2b** are similar to those of the copper(II) carboxylates which have the classical copper(II) acetate-type structure.[5] While the crystal structure of **2b** has not been determined, the structure is certainly more closely related to complexes with a square pyramidal metal geometry than **1** and **2a**.

Further evidence which supports the above conclusion, that crystal packing forces play an important role in determining the geometry around copper(II) in **1** and **2a**, is provided by magnetic-moment data (see Table 11). Crystalline **1** and powder **2a** have the same magnetic moments at 308 K, 1.68 μ_B, both of which have similar magnetic properties that are consistent with a distorted trigonal bipyramidal structure around each copper(II) in which there is one very long Cu–O bond (2.3—2.5 Å), vide supra. The magnetic moments of these complexes in benzene solution at the same temperature are 1.56 μ_B and 1.53 μ_B, respectively. This decrease in the magnetic moments towards the value obtained for crystalline **2b** (1.51 μ_B), for which magnetic measurements are consistent with a cage structure more closely aligned with the copper(II) acetate type, suggests that on dissolution in benzene the forces which cause the molecular distortion are diminished.

The question arises as to what is structurally different

Table 11. Comparison of the Magnetic Properties of $Cu(O_2CCPh_3)_2\cdot n$ py Complexes at 308 K

Complex	$\chi_A\times10^6$ / emu mol^{-1}	μ_{eff} / μ_B	Form
1	1150[a,b]	1.68	Cryst
	1047[c]	1.56	Soln, C_6H_6
2a[d]	1150[a,b]	1.68	Powder
	1011[c]	1.53	Soln, C_6H_6
2b	930[a,b]	1.51	Cryst
3	1390[b,e]	1.85	Cryst

a) Corrected for constituent atom diamagnetism and temperature independent paramagnetism, 60×10^{-6} emu mol^{-1} of Cu(II). b) Calculated from variable temperature data, Faraday method. c) Evans method; not corrected for paramagnetic impurities. d) Prepared by Procedure 1. e) Corrected for temperature independent paramagnetism of Cu(II).

about the bridging triphenylacetato ligand which leads to the structural transformation. The triphenylacetato ligand is bulkier than other carboxylato ligands in complexes $[Cu_2(O_2CR)_4(py)_2]$ of known structure.[5] An examination of a model of **1** based on crystal-structure data, reveals that there is an area of space around each of the pyridine rings which is void of atoms. Thus, more efficient crystal packing can be obtained if the pyridine rings are angled away from the apical positions to make room for the pyridine rings on adjacent dimer units.

At the same time, the intramolecular forces between the bulky bridging triphenylacetato ligands may also have some effect on the structure. Steric repulsions between the bridging ligands could be reduced by staggering two adjacent triphenylacetato ligands with respect to the horizontal plane in D_{4h} symmetry. The out-of-plane ligands, i.e., the ligands which form the long bridges (which have right-handed conformations of the phenyl groups) show the largest deviations from threefold symmetry. These observations suggest that intramolecular steric forces could be responsible for some of the staggering of the ligands, as well as for the larger deviations from threefold symmetry. Porter et al.[12] have suggested that intramolecular steric crowding is responsible for determining the copper coordination geometry in the copper(II) trichloroacetate complexes. However, intramolecular steric crowding cannot be the major factor which controls the geometry of the dimeric copper(II) triphenylacetate–pyridine complexes, since all indications are that the structure of complex **2b** is closely akin to the classical copper(II) acetate monohydrate type.

Recently, crystal structures have been reported for the complexes, $[Cu_2(O_2CMPh_3)_4(L)_2]$ (where M=Si, L=α-picoline; M=Ge, L=quinoline), both of which have carboxylato ligands with three α-phenyl groups.[49] It is interesting to note that these complexes, while maintaining the square pyramidal metal geometry, show considerably more variation in the Cu–O bond distances than observed for complexes in which the carboxylato ligand has fewer than three α-phenyl groups. On inspection, their structures show a slight distortion of the type observed for **1**, resulting in one slightly longer Cu–O bonds to each copper in the adjacent bridging groups. One would expect less distortion by intramolecular forces in silicon and germanium complexes than in **1** as a result of the longer C–M distances in the carboxylato ligands.

The 1:2 dark blue crystalline complex, $Cu(O_2CCPh_3)_2 \cdot 2py$ (**3**), is formed from **1** by placing the blue-green crystals of **1** in an ethanol–pyridine solution and allowing the reaction to proceed for several days. The interesting aspect of this conversion is that it appears to occur in the solid phase. After one day, mixed crystals are obtained which contain both blue-green and dark-blue areas.[50] Apparently, pyridine molecules are able to diffuse into the crystal, perhaps replacing the benzene of crystallization, where the reaction occurs. Crystal-packing maps of **1** indicate that there is considerable space between molecular units. It is interesting to note that the volume of the unit cell for **3** is about one-half the volume of **1** with the *a* unit-cell distance in **3** being about one-half the *b* distance in **1**, while the other unit cell distances are comparable.

The structure of $Cu(O_2CCPh_3)_2 \cdot 2py$ (**3**) is a variation of the *trans*-bis(acetato-*O,O'*)diamminecopper(II) type.[35] Several other structures of this type, $Cu(O_2CR)_2 \cdot 2L$, where L is a nitrogeneous base, have been reported.[51–54] In comparing **3** with these structures, one observes that the Cu–O(2) distance (2.673 Å) is the shortest and the N–Cu–O(2) angle (81.0°) is the smallest so far reported. Also, the N–Cu–O(1) angle (91.5°) is greater than 90°, indicating a small deviation from a square planar arrangement of the atoms around copper in the coordination plane. In the other complexes of this type, the angles corresponding to the N–Cu–O(2) angle are close to 90° except for $Cu(O_2CCH_3)_2$(imidazole)$_2$ (86°) where intermolecular hydrogen bonding occurs between imidazole and O(2).[12] These data indicate that in **3** the steric effects resulting from the bulky triphenylmethyl groups cause a twisting of the carboxyl groups relative to the coordination plane around copper.[55] The dihedral angle between the carboxyl ligand and the coordination plane is 78.0°.

Davey and Stephens[56] have reported the crystal structure for $Cu(O_2CCHCl_2)_2$(α-picoline)$_2$. In this complex, the *cis* conformation of the α-picoline ligands results in an asymmetric arrangement of the chelating dichloroacetato ligands. The geometry around copper(II) is distorted from a square planar arrangement, the angles formed by the out-of-plane Cu–O bonds with the plane are different, and the out-of-plane Cu–O distances vary.

In conclusion, the geometry of the coordination sphere around copper in monomeric and dimeric copper(II) carboxylates can vary considerably, depending on the size and shape of the ligands. Crystal packing forces and intramolecular repulsion forces are responsible for these structural changes. The flexibility of the coordination sphere around copper(II) has been noted.[12,36,40] Thus, one would expect to find other variations from the classical copper(II) acetate monohydrate-type and the *trans*-bis(acetato-*O,O'*)diamminecopper(II)-type structures as the spatial relationships both within and between the molecules are changed.

We greatfully acknowledge the contributions of Professor Y. Saito and Dr. S. Ohba, Keio University, for their fruitful discussions and suggestions in the preparation of this paper. We also wish to thank Professor D. W. Pratt, University of Pittsburgh, for the use of his ESR facilities, Drs. I. B. Goldberg and T. M. McKinney, Rockwell International, for running the ESR spectra of **2b**, and Professor J. W. Whittaker, Carnegie-Mellon University, for running an ESR spectrum of **2a**. The authors also wish to acknowledge Dr. C. E. Taylor's (formerly of our group) contribution in determining the magnetic moments by the Evans method.

References

1) Presented in part at the 23rd International Conference on Coordination Chemistry, Boulder, CO, July 29—Aug. 3 1984.

2) D. H. Hendrickson, "Magneto-Structural Correlations in Exchange Coupled Systems," ed by R. D. Willett, D. Gatteschi, and O. Kahn, D. Reidel Publishing Co., Dordrecht (1985), pp. 523—554.

3) J. Catterick and P. Thornton, *Adv. Inorg. Chem. Radiochem.*, **45**, 291 (1977).

4) R. J. Doedens, *Prog. Inorg. Chem.*, **21**, 209 (1976).

5) M. Melnik, *Coord. Chem. Rev.*, **42**, 259 (1982).

6) R. C. Mehrotra and R. Bohra, "Metal Carboxylates," Academic Press, London (1983), pp. 286—295.

7) Chang, C.-H. Ph. D. Thesis, University of Pittsburgh, Pittsburgh, PA, 1982; *Diss. Abstr. B*, **43**, 1467B, (1982).

8) O. W. Steward, M. Kato, S.-C. Chang, M. Sax, C.-H. Chang, T. Taura, C. F. Jury, Y. Muto, T. Tokii, J. F. Pletcher, and C. S. Yoo, 23rd International Conference on Coordination Chemistry, Boulder, CO, July 29—Aug. 3 1984, Abstr., p. 247.

9) M. Yamanaka, S. Ohba, Y. Saito, O. W. Steward, M. Kato, T. Tokii, Y. Muto, and I. Suzuki, 39th Symposium on Coordination Chemistry, Mito, Japan, Sept. 26—28 1989, Abstr., 1BP02.

10) M. Kato and Y. Muto, *Coord. Chem. Rev.*, **92**, 45 (1988).

11) L. C. Porter, M. H. Dickman, and R. J. Doedens, *Inorg. Chem.*, **22**, 1962 (1983).

12) L. C. Porter, M. H. Dickman, and R. J. Doedens, *Inorg. Chem.*, **25**, 678 (1986).

13) Y. Muto, M. Nakashima, T. Tokii, M. Kato, and I. Suzuki, *Bull. Chem. Soc. Jpn.*, **60**, 2849 (1987).

14) H. Uekusa, S. Ohba, Y. Saito, O. W. Steward, M. Kato, T. Tokii, and Y. Muto, 39th Symposium on Coordination Chemistry, Mito, Japan, Sept. 26—28 1989, Abstr., 1BP01.

15) H. Horie, S. Husebye, M. Kato, E. A. Meyers, Y. Muto, I. Suzuki, T. Tokii, and R. A. Zingaro, *Acta Chem. Scand. A*, **40**, 579 (1986).

16) H. Uekusa, S. Ohba, Y. Saito, T. Tokii, Y. Muto, M. Kato, S. Husebye, and O. W. Steward, 28th International Conference on Coordination Chemistry, Gera, GDR, Aug. 3—18 1990, Abstr., 6—33.

17) O. W. Steward, R. C. McAfee, S.-C. Chang, S. R. Piskor, W. J. Schreiber, C. F. Jury, C. E. Taylor, J. F. Pletcher, and C.-S. Chen, *Inorg. Chem.*, **25**, 771 (1986).

18) The benzene of crystallization is easily lost from the crystals; therefore, the analysis can vary depending on how the crystals are dried.

19) W. H. Zachariasen, *Acta Crystallogr.*, **16**, 1139 (1963).

20) P. Main, S. E. Hall, L. Lessinger, G. Germain, J. P. Declercq, and M. M. Woolfson, "MULTAM 78, A System of Computer Programs for the Automatic Solutions of Crystal Structures from X-Ray Diffraction Data," University of York, England (1987).

21) W. Furey, Jr., B. C. Wang, and M. Sax, *J. Appl. Crystallogr.*, **15**, 160 (1982).

22) R. Shiono, Tech. Rep. No. 48, Crystallography Department, University of Pittsburgh, Pittsburgh, PA.

23) a) "International Tables for X-Ray Crystallography," Kynoch Press, Birmingham (1974), Vol. III. b) R. F. Stewart, E. R. Davidson, and W. T. Simpson, *J. Chem. Phys.*, **42**, 3175 (1965).

24) Tables of observed and calculated structure factors, positional parameters for the hydrogen atoms, anisotropic thermal parameters, bond distances and angles, least-squares planes, torsion angles, nonbonding intramolecular distances for **1** and **3** along with a stereoscopic ORTEP packing diagram of **3** are deposited as Document No. 8963 at the Office of the Editor of Bull. Chem. Soc. Jpn.

25) R. A. Lalancette, M. Cefola, W. C. Hamilton, and S. J. LaPlaca, *Inorg. Chem.*, **6**, 2127 (1967).

26) Recorded on a Bruker model ER-300 ESR spectrometer.

27) Recorded on a Bruker model 220D ESR spectrometer with a 031 microprocessor field controller equipped with an Eldorado model 989 frequency counter. Temperature was controlled via a modified Varian TE "Dual" cavity equipped with a Varian Dewer insert and a model V-4540 temperature controller.

28) P. W. Selwood, "Magnetochemistry," Interscience, New York (1956), pp. 78, 91.

29) E. K. Hyde, G. Gordon, and G. F. J. Kokoszka, *Inorg. Nucl. Chem.*, **30**, 2155 (1968).

30) T. Nakagawa (University of Tokyo) and Y. Oyanagi (University of Tsukuba), SALS (model D).

31) Data for the least-squares planes are listed in Table 4S. The average estimated standard deviation of the atoms from the planes is 0.003 Å.

32) This range is much larger than is reported for complexes with the copper(II) acetate monohydrate-type structure, Ref. 5.

33) J. Zemann, *Z. Anorg. Allg. Chem.*, **324**, 241 (1963).

34) G. A. Jeffery and A. Robbins, *Acta Crystallogr., Sect. B*, **36**, 1820 (1980).

35) Yu. A. Simonov, A. V. Ablov, and T. I. Malinovski, *Kristallografiya*, **8**, 270 (1963).

36) N. Ray, L. Hulett, R. Sheahan, and B. Hathaway, *Inorg. Nucl. Chem. Lett.*, **14**, 305 (1978).

37) E. Wasserman, L. C. Snyder, and W. A. Yager, *J. Chem. Phys.*, **41**, 1763 (1964).

38) T. D. Smith and J. R. Pilbrow, *Coord. Chem. Rev.*, **13**, 173 (1974).

39) H. J. Price, J. R. Pilbrow, K. S. Murray, and T. D. Smith, *J. Chem. Soc. A*, **1970**, 968.

40) B. J. Hathaway and D. E. Billing, *Coord. Chem. Rev.*, **5**, 143 (1970).

41) A. B. P. Lever, "Inorganic Electronic Spectroscopy," 2nd ed, Elsevier, Amsterdam (1984), pp. 554—572.

42) R. W. Jotham, S. F. A. Kettle, and J. A. Marks, *J. Chem. Soc., Dalton Trans.*, **1972**, 428.

43) S. R. Desjardins, D. E. Wilcox, R. L. Musselman, and E. I. Solomon, *Inorg. Chem.*, **26**, 288 (1987).

44) P. K. Ross, M. D. Allendorf, and E. I. Solomon, *J. Am. Chem. Soc.*, **111**, 4009 (1989).

45) K. Nakamoto, "Infrared and Raman Spectra of Inorganic and Coordination Compounds," 4th ed, Interscience, New York (1986), pp. 231—233.

46) R. C. Mehrotra and R. Bohra, "Metal Carboxylates," Academic Press, London (1983), pp. 48—60.

47) S. Emori, K. Ohishi, H. Kurihara, and Y. Muto, *Bull. Chem. Soc. Jpn.,* **61**, 4439 (1988).

48) L. Pauling, "The Nature of the Chemical Bond," 3rd ed, Cornell University Press, Ithaca (1960), p. 262.

49) H. Uekusa, S. Ohba, Y. Saito, M. Kato, O. W. Steward, T. Tokii, and Y. Muto, *Acta Crystallogr., Sect. C,* **46**, 1805 (1990).

50) The first crystal on which diffraction data were collected to determine the structure of **3** turned out to be a mixed crystal.

51) G. Davey and F. S. Stephens, *J. Chem. Soc. A,* **1971**, 1917.

52) H. A. Henriksson, *Acta Crystallogr. Sect. B,* **33**, 1947 (1977).

53) N. E. Heimer and L. Y. Ahmed, *Inorg. Chem. Acta,* **64**, L65, (1982).

54) A. Busnot, F. Busont, A. Laclaire, and M. Bernard, *Z. Anorg. Allg. Chem.,* **503**, 207 (1983).

55) The intramolecular distances between the ligands in **3** of <3.8 Å are given in Table 10S.

56) G. Davey and F. S. Stephens, *J. Chem. Soc. A,* **1971**, 2578.